Received: 20 February 2024 | Accepted: 17 July 2024

DOI: 10.1111/head.14825

RESEARCH SUBMISSIONS

Role of diffusion tensor imaging in the evaluation of white matter integrity in idiopathic intracranial hypertension

Bahar Atasoy MD[1] | Asli Yaman Kula MD[2] | Serdar Balsak MD[1] | Yagmur Basak Polat MD[1] | Zeynep Donmez MD[1] | Ahmet Akcay MD[1] | Abdusselim Adil Peker MD[1] | Ozlem Toluk PhD[3] | Alpay Alkan MD[1]

[1]Department of Radiology, Bezmialem Vakıf University Hospital, Istanbul, Turkey

[2]Department of Neurology, Bezmialem Vakıf University Hospital, Istanbul, Turkey

[3]Department of Biostatistics and Medical Informatics, Bezmialem Vakıf University Hospital, Istanbul, Turkey

Correspondence
Bahar Atasoy, Department of Radiology, Faculty of Medicine, Bezmialem Vakif University, Istanbul 34093, Turkey.
Email: bahar_atasoy@hotmail.com

Abstract

Objectives: To determine whether idiopathic intracranial hypertension (IIH) may affect white matter integrity and optic pathways by using diffusion tensor imaging (DTI) and to correlate the DTI metrics with intracranial pressure (ICP).

Methods: This study is a retrospective case–control study. A total of 42 patients who underwent lumbar puncture and those with elevated ICP, meeting the diagnostic criteria for IIH, were included in the study. All patients had supportive magnetic resonance imaging findings for the diagnosis of IIH. The headache control group comprised 36 patients who presented to the Neurology Department with infrequent episodic tension-type headache, had a normal neurologic examination, and had clinical and radiological findings suggestive of normal ICP. For each patient with IIH, clinical findings and ophthalmological measurements were recorded. The apparent diffusion coefficient (ADC), fractional anisotropy (FA), axial diffusivity (AD), and radial diffusivity (RD) values were calculated using a region of interest-based method in different white matter tracts and optic pathways and compared.

Results: A total of 42 patients diagnosed with IIH (three males, 39 females), with a mean (standard deviation [SD] age of 38.1 (8.9) years), and 36 headache controls (10 males, 26 females, mean [SD] age; 38.1 [9.4] years) were included in the study. The mean (SD) body mass index (BMI) of the patients with IIH was 25.2 (1.9) kg/m^2, and the mean (SD) BMI of the headache controls was 23.3 (1.5) kg/m^2 ($p < 0.001$). Decreased FA values and increased RD values in the cingulum were detected in patients with IIH compared to the headache controls ($p = 0.003$, Cohen's $d = 0.681$; $p = 0.002$ Cohen's $d = -0.710$). Decreased AD values in the left and right superior cerebellar peduncle and increased ADC values in the middle cerebellar peduncle were detected in patients with IIH compared to the headache controls ($p < 0.001$, Cohen's $d = 0.961$; $p = 0.009$, Cohen's $d = 0.607$; $p = 0.015$, Cohen's $d = -0.564$). Increased ADC and RD values and decreased FA values in optic nerve were detected in patients with IIH ($p = 0.010$, Cohen's $d = -0.603$; $p = 0.004$, Cohen's $d = -0.676$; $p = 0.015$ Cohen's $d = 0.568$). A positive correlation was found between the cerebrospinal fluid pressure and ADC

Abbreviations: AD, axial diffusivity; ADC, apparent diffusion coefficient; BMI, body mass index; CI, confidence interval; CSF, cerebrospinal fluid; DTI, diffusion tensor imaging; FA, fractional anisotropy; ICP, intracranial pressure; IIH, idiopathic intracranial hypertension; IQR, interquartile range; LP, lumbar puncture; MD, mean deviation; MRI, magnetic resonance imaging; NPH, normal pressure hydrocephalus; PSD, pattern standard deviation; RD, radial diffusivity; RNFL, retinal nerve fiber layer; ROI, region of interest; SD, standard deviation.

values of the left and right superior and left inferior longitudinal fasciculus, genu of the corpus callosum, and right optic radiation ($r=0.43$, $p=0.005$; $r=0.31$, $p=0.044$; $r=0.39$, $p=0.010$; $r=0.35$, $p=0.024$; $r=0,41$, $p=0.007$). There was a positive correlation between the retinal nerve fiber layer thickness and the ADC values of the optic nerve ($r=0.32$, $p=0.039$).

Conclusions: Intracranial hypertension can be associated with deteriorated DTI values, which might be interpreted as a sign of impaired white matter microstructural integrity in many brain regions beyond the periventricular white matter. Pressure-induced edema and axonal degeneration may be the potential underlying mechanisms of this microstructural damage.

Plain Language Summary

Females of reproductive age with obesity are disproportionately affected by idiopathic intracranial hypertension (IIH), and the incidence of this diagnosis is increasing along with the prevalence of obesity. We do not yet understand how IIH develops, but dysregulation of intracranial pressure is an important area of research interest, so we hypothesized that increased intracranial pressure may affect white matter microstructure and optic pathways in patients with IIH. Using data from a specialized imaging technique, we found that patients with IIH may have impaired white matter microstructural integrity in several areas of the brain and microstructural alterations in the optic nerve.

KEYWORDS
apparent diffusion coefficient, diffusion tensor imaging, fractional anisotropy, idiopathic intracranial hypertension, optic pathways

INTRODUCTION

Idiopathic intracranial hypertension (IIH) is a syndrome characterized by elevated intracranial cerebrospinal fluid (CSF) pressure without any identifiable cause, such as hydrocephalus or causative mass.[1,2] Females of reproductive age with obesity are by far the most typically affected demographic; nevertheless, the exact cause of this condition remains unknown.[3] According to current estimates, there are 0.03–2.36 instances of IIH per 100,000 people in the general population[3–8]; however, the incidence of this diagnosis is increasing along with the prevalence of obesity.[9]

Headaches, vision problems (either temporary or permanent visual loss), photophobia, pulsatile tinnitus, and/or eye pain are the most common complaints encountered in patients with IIH.[9,10] The distinctive finding on fundoscopic examination is papilledema, which is usually bilateral but can occasionally be unilateral or absent, making the clinical diagnosis challenging.[11] The neurological evaluation is frequently normal, except for occasional cases of sixth cranial nerve palsy or visual field deficiency. For individuals suspected of having IIH, brain imaging using magnetic resonance imaging (MRI) is necessary to rule out other possible causes of increased CSF pressure, such as brain tumors, dural sinus thrombosis, or hydrocephalus. On MRI, the following imaging characteristics help to support the diagnosis of IIH: prominent subarachnoid space around the optic nerves, flattening of the posterior sclera, partially empty sella turcica, enlarged Meckel cave, and bilateral venous sinus stenosis.[10–14]

Diffusion tensor imaging (DTI) is a non-invasive MRI diagnostic technique for detecting microstructural changes in the cerebral white matter based on the diffusion characteristics of water. DTI provides information about the microstructural changes at the cellular level in the brain, and due to this feature, it might identify microstructural deterioration before the conventional MRI findings.[15–17] Fractional anisotropy (FA), apparent diffusion coefficient (ADC), radial diffusivity (RD), and axial diffusivity (AD) are the four metrics derived from DTI that are used to assess the diffusion properties of tissues. FA values provide important information about the microstructure of white matter, fiber density, axon diameter, and myelination. ADC values provide important information about tissue cellularity and edema. To the best of our knowledge, there are very few DTI studies in the literature that evaluate the optic pathways and white matter microstructure in patients with IIH. These DTI studies pointed out the microstructural changes in periventricular white matter and optic nerves.[2,17,18]

We hypothesized that increased intracranial pressure (ICP) might affect white matter microstructure and optic pathways in patients

with IIH. The study's objective was to examine the impact of elevated ICP on the microstructural characteristics of optic pathways and white matter by using DTI in patients with IIH and to establish a correlation between the DTI results and CSF opening pressure to potentially uncover microscopic changes that could further our understanding of the condition.

METHODS

Participants

This was a retrospective cross-sectional study. The study was approved by the ethical committee of Bezmialem Foundation University, Turkey (E-54022451-050.05.04-127892) and performed according to the ethical standards of the Declaration of Helsinki. Written informed consent was obtained from all the participants. The MRI and clinical data of the patients admitted to the Bezmialem Foundation University Neurology Department between 2017 and 2022 were retrospectively analyzed.

Patients who presented to the Neurology Department with headaches were analyzed. A total of 42 patients who underwent lumbar puncture (LP) to elucidate the etiology, those with elevated ICP, and those who met the diagnostic criteria for IIH according to the Modified Dandy Criteria (International Classification of Diseases Ninth revision Clinical Modification; 348.2 Benign Intracranial Hypertension) were included in the study. The participants underwent brain MRI before LP. All patients had supportive MRI findings for the diagnosis of IIH. A total of 122 potential participants were assessed for eligibility for the study. The participants with missing clinical data ($n=11$), T2 hyperintense lesions on MRI ($n=16$), poor quality of DTI due to motion artifacts ($n=$nine), no LP performed ($n=$five), and no brain MRI was performed before LP ($n=$eight) were excluded from the study ($n=49$). Moreover, participants who did not fulfill the Modified Dandy Criteria for IIH ($n=31$) were excluded from the study. A flow diagram for the included and excluded patients is provided in Figure 1. The headache control group comprised 36 patients who presented to the Neurology Department with infrequent episodic tension-type headache, had a normal neurologic examination, and had clinical and radiological findings suggestive of normal ICP. The headache control group with tension-type headache met the International Classification of Headache Disorders, third edition criteria. LP was not performed on the headache control group. All participants had no evidence of white matter hyperintensities on brain MRI. For each patient, sex, age, ICP values, and medical history, including symptoms of headache, nausea, blurry vision, diplopia, dizziness, tinnitus, transient visual obscurations, and papilledema, were recorded.

The fundus evaluation of the patients with IIH was performed according to the Frisen staging scale, and the grades of the papilledema of each eye were recorded. Ophthalmological measurements were made in both eyes of each patient with IIH by the experienced ophthalmologist in our ophthalmology clinic. The retinal nerve fiber layer (RNFL) thickness of each eye was automatically calculated and recorded in micrometers (μm) using optical coherence tomography. In addition, visual field examinations were performed, and each eye's mean deviation (MD) and pattern standard deviation (SD) values were recorded.

The MRI protocol

The MRI was performed using a 1.5-T Siemens Avanto SQ-Engine (Siemens, Erlangen, Germany). All images were acquired using an eight-channel head coil. Routine brain MRI protocol and DTI were performed for all participants.

The DTI protocol comprised a single-shot spin-echo echo-planar sequence with fat suppression technique with the following parameters: repetition time/echo time = 3400/85 ms; field of view, 230 mm; slice thickness, 5 mm; matrix, 128 × 128; voxel size, 1.8 × 1.8 × 4 mm; the number of signals averaged, 1; bandwidth 1502 Hz/px. The 30 diffusion-encoding directions were used at $b=0\,s/mm^2$ and $b=1000\,s/mm^2$. Parallel imaging using generalized autocalibrating partially parallel acquisition (GRAPPA) with an integrated parallel acquisition technique (iPAT) factor of 3 was applied. The processing of the DTI data was performed on the workstation with "syngo.via" (Siemens, Erlangen, Germany). The ADC, FA, AD, and RD maps were reconstructed.

T1-weighted three-dimensional Magnetization-Prepared Rapid Acquisition Gradient Echo (3D-MPRAGE) and T2-wieghted images were used as anatomic references for the placement and tracing of the regions of interest (ROIs) throughout the following different white matter tracts and optic pathways: right and left cingulum (R_CG, L_CG), right and left corona radiata (R_CR, L_CR), genu and splenium of corpus callosum (GCC, SCC), right and left superior longitudinal fasciculus (R_SLF, L_SLF), right and left inferior longitudinal fasciculus (R_ILF, L_ILF), right and left inferior frontooccipital fasciculus (R_IFOF, L_IFOF), right and left anterior limb of internal capsule (R_ALIC, L_ALIC), right and left posterior limb of the internal capsule (R_PLIC, L_PLIC), at the mid-pontine level right and left superior cerebellar peduncle (R_SCP, L_SCP), and right and left middle cerebellar peduncle (R_MCP, L_MCP). Moreover, optic pathways, including right and left optic nerve (R_ON, L_ON), right and left optic radiation (R_OR, L_OR), and right and left calcarine sulcus, were assessed (Figures 2–4).

One neuroradiologist (B.A.), who was blinded to the diagnosis, carried out the placement and size adaptation of all ROIs. The ADC, FA, AD, and RD values were automatically calculated, and the mean values for each metric were recorded for assessment.

Statistical analysis

This is the primary analysis of the previously collected data. Taking previous studies as a reference and using a correlation coefficient

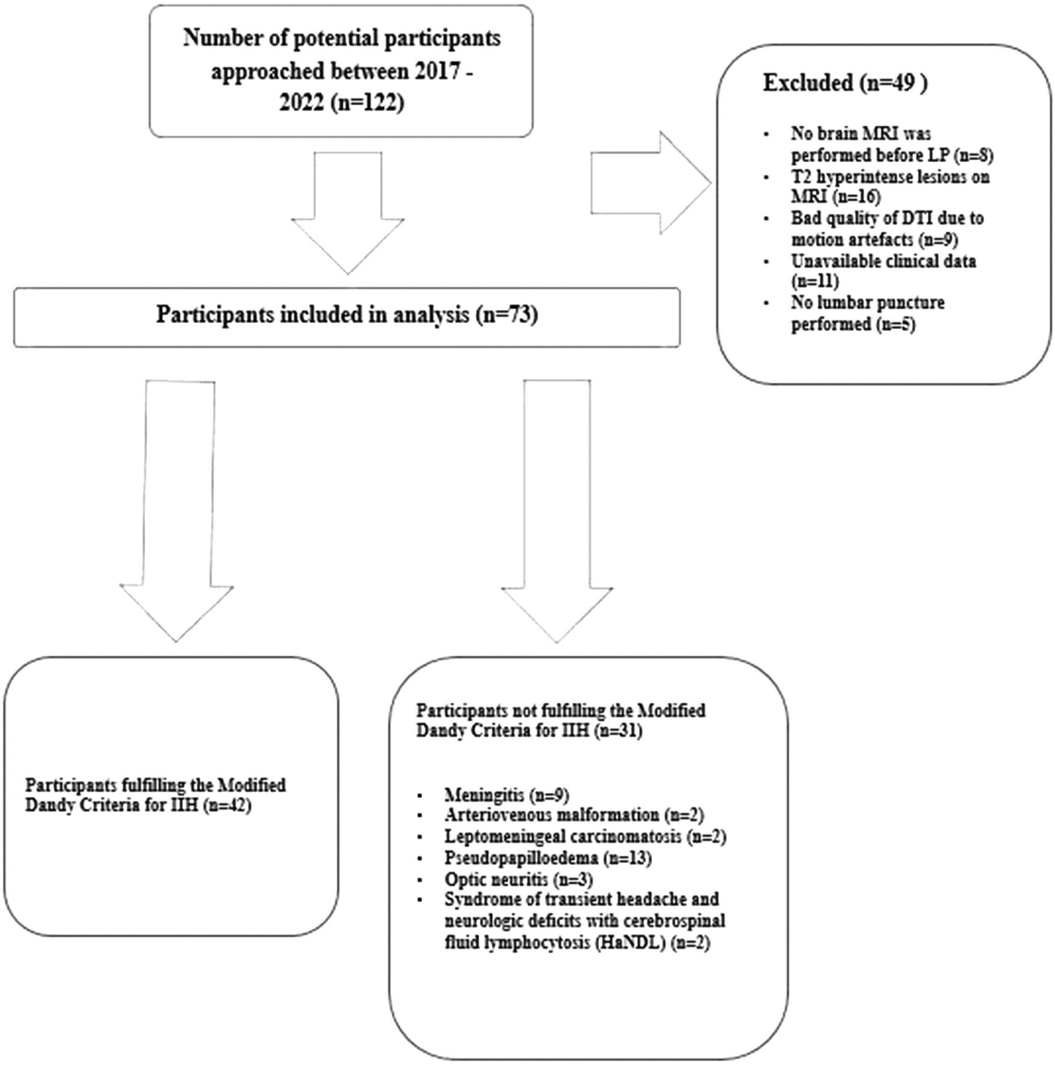

FIGURE 1 Flow diagram for the included and excluded patients with idiopathic intracranial hypertension (IIH). DTI, diffusion tensor imaging; LP, lumbar puncture; MRI, magnetic resonance imaging.

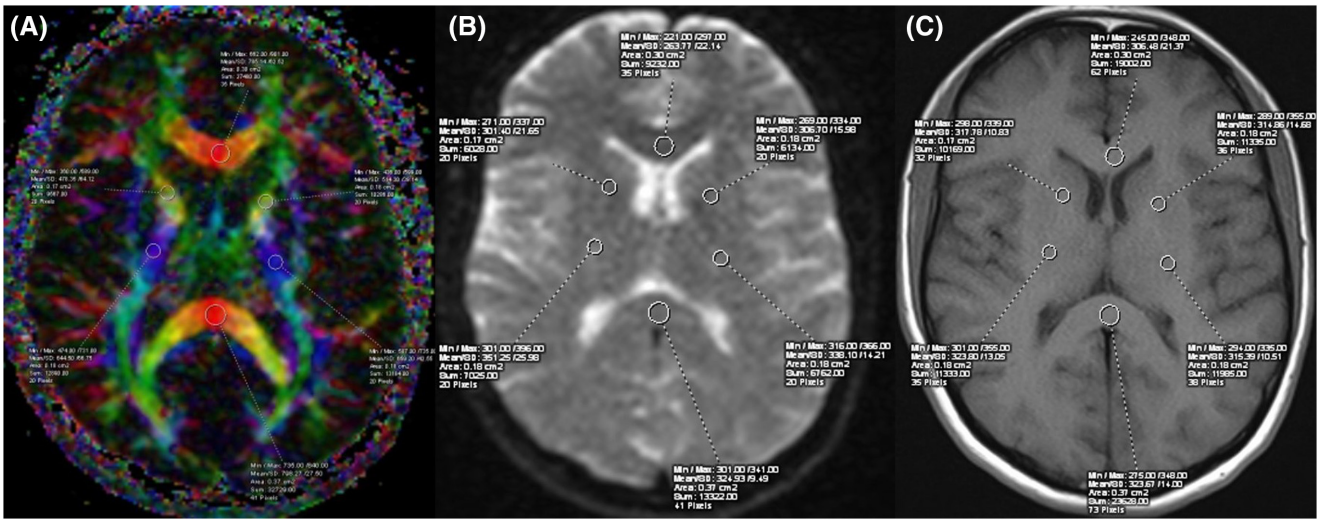

FIGURE 2 Placement of the region of interests (ROIs) on the corpus callosum genu and splenium, right and left anterior and posterior limb of internal capsule on directionally color-coded map (A) and anisotropy map (B). T1-weighted images (C) were used as anatomic references for the placement of the ROIs. [Color figure can be viewed at wileyonlinelibrary.com]

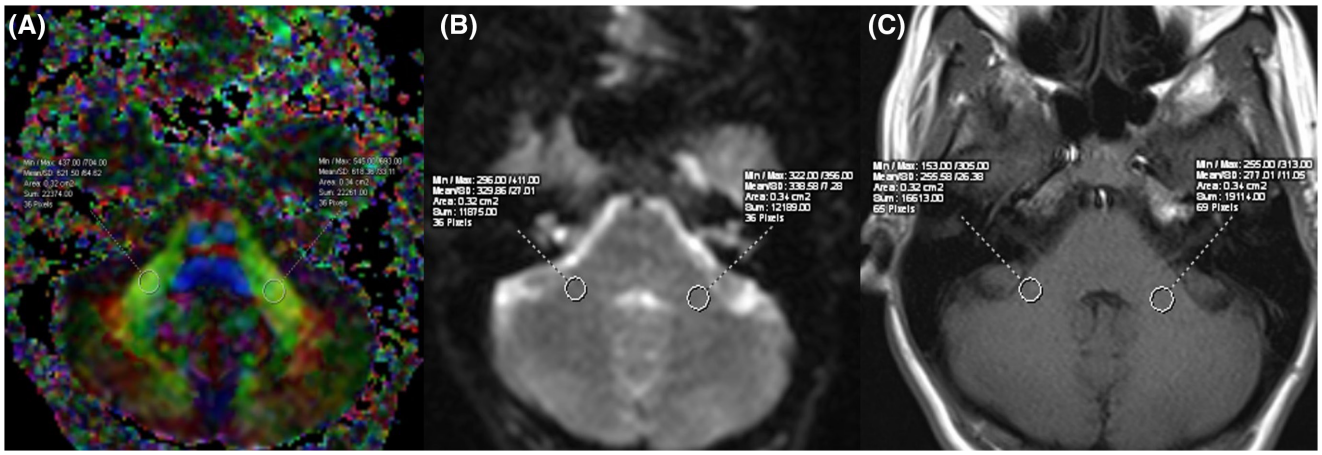

FIGURE 3 Placement of the region of interests (ROIs) on the right and left middle cerebellar peduncle on directionally color-coded map (A) and anisotropy map (B). T1-weighted images (C) were used as anatomic references for the placement of the ROIs. [Color figure can be viewed at wileyonlinelibrary.com]

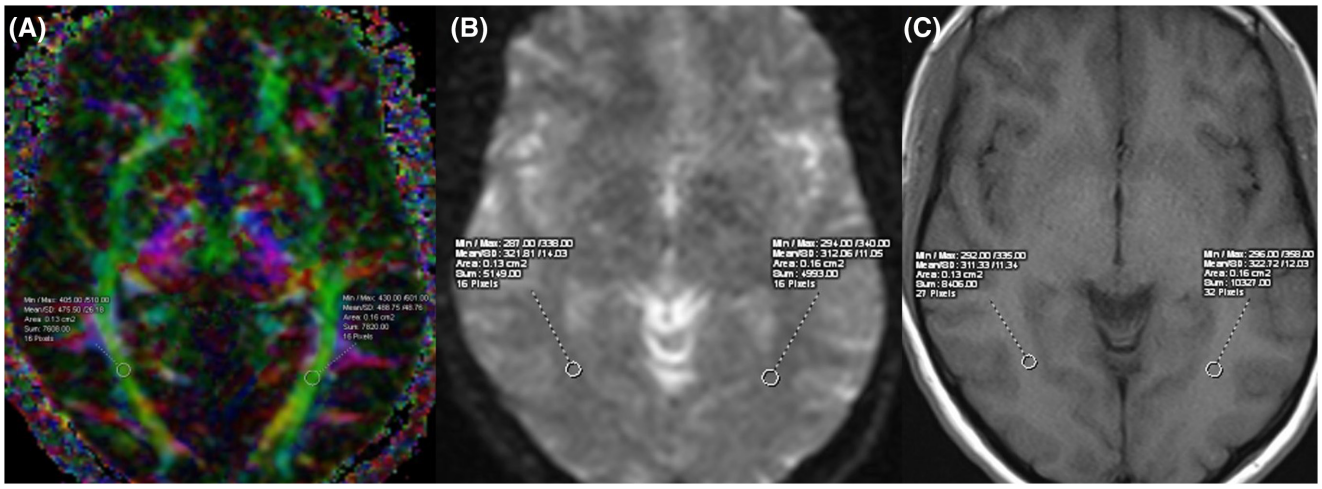

FIGURE 4 Placement of the region of interests (ROIs) on the right and left optic radiation on directionally color-coded map (A) and anisotropy map (B). T1-weighted images (C) were used as anatomic references for the placement of the ROIs. [Color figure can be viewed at wileyonlinelibrary.com]

$r = -0.216$ for 80% power at a 95% confidence level, the minimum number of samples was found to be 16. Power analysis was calculated with PASS 2008 software.

Variables' normal or non-normal distributions were evaluated with the Shapiro–Wilk test. Descriptive statistics were presented as mean and standard deviation (SD) for normally distributed continuous data, median (25th–75th percentile, interquartile range [IQR]) for non-normally distributed continuous data, and frequencies with percentages for categorical data. Group comparisons were analyzed using the independent samples *t*-test. ADC, FA, RD, and AD relationships were examined with the Pearson correlation coefficient. Additionally, Cohen's *d* effect sizes were presented. Categorical variables were analyzed with Pearson chi-square test. The Statistical Package for the Social Sciences (SPSS) version 28.0 (IBM Corp. Armonk, NY, USA) and MedCalc version 19.6.1 software were used for analysis. All hypothesis tests were two-tailed. The Benjamini–Hochberg false discovery rate method was applied for multiple comparisons. After this correction, the threshold for statistical significance was set at $p < 0.0153$. The Spearman correlation coefficient was used to assess the correlation between the ophthalmological measurements and DTI parameters.

RESULTS

Demographics and clinical characteristics of the patients with IIH

A total of 42 patients diagnosed as IIH (Group 1; three male, 39 female, mean [SD] age 38.1 [8.9] years) and 36 headache controls (Group 2; 10 male, 26 female, mean [SD] age 38.1 [9.4] years) were included. The mean (SD) body mass index (BMI) of the patients with IIH was 25.2 (1.9) kg/m^2, and the mean (SD) BMI of the headache controls was 23.3 (1.5) kg/m^2 in our study. There was a statistically significant difference between the BMI values of the patients with IIH and headache controls in our study ($p < 0.001$).

The most common symptom was headache (95%, $n=40$). Other symptoms included nausea (23%, $n=10$), dizziness (14%, $n=$six), tinnitus (26%, $n=11$), transient visual obscuration (19%, $n=$eight), blurred vision (43%, $n=18$), diplopia (5%, $n=$two). Bilateral papilledema was detected in 31 (73%) patients. The median (IQR) CSF opening pressure was 350.00 (300.00–390.00) mm.

The IIH group's ocular MRI findings included posterior optic globe flattening (92%, $n=39$), optic nerve head protrusion (38%, $n=16$), and optic nerve tortuosity (90%, $n=38$).

Ophthalmological measurements

Regarding the grade of papilledema in the right eyes, 36% ($n=15$) of patients had Grade 0, 26% ($n=11$) of patients had Grade I, 21% ($n=$nine) of patients had Grade II, and 7% ($n=$three) of patients had Grade III, and of patients, 10% ($n=$four) had Grade IV Frisen grade of papilledema. As for the left eyes, 31% ($n=13$) of patients had Grade 0, 33% ($n=14$) of patients had Grade I, 21% ($n=$nine) of patients had Grade II, and 5% ($n=$two) of patients had Grade III, and of patients, 10% ($n=$four) had Grade IV Frisen grade of papilledema.

According to the optical coherence tomography results, the median (IQR) RNFL thickness of the worst affected eye was 110.5 (104–136) μm.

After visual field examinations, the median (IQR) MD value of the worst affected eye was −4.58 (−6.82 to −3.64) dB.

The median (IQR) pattern SD (PSD) value of the worst affected eye was 2.80 (2.37–6.15) dB. The ophthalmological measurements are presented in the Table S1.

The demographic variables and clinical data are summarized in Table 1.

Comparison of DTI results between the 42 patients with IIH and 36 headache controls

The left cingulum FA values were significantly lower in headache controls compared to patients with IIH (Cohen's $d=0.681$, 95% confidence interval [CI] 18.68–88.74; $p=0.003$). The left cingulum RD values were significantly higher in headache controls compared to patients with IIH (Cohen's $d=-0.710$, 95% CI −83.72 to −18.57; $p=0.002$).

The right anterior limb internal capsule FA values were significantly lower in headache controls compared to patients with IIH (Cohen's $d=0.454$, 95% CI 0.11–56.11; $p=0.049$). The right anterior limb internal capsule RD values were significantly higher in headache controls compared to patients with IIH (Cohen's $d=-0.506$, 95% CI −52.28 to −2.90; $p=0.029$).

The left superior cerebellar peduncle AD and right superior cerebellar peduncle AD values were significantly lower in headache controls compared to patients with IIH (Cohen's $d=0.961$, 95% CI 89.19–247.93, $p<0.001$; Cohen's $d=0.607$, 95% CI 26.33–180.13, $p=0.009$, respectively).

The left middle cerebellar peduncle ADC values were significantly higher in headache controls compared to patients with IIH (Cohen's $d=-0.564$, 95% CI −39.04 to −4.28; $p=0.015$).

The left optic nerve ADC values were significantly higher in headache controls compared to patients with IIH (Cohen's $d=-0.603$, 95% CI −212.40 to −30.33; $p=0.010$). The left optic nerve FA values were significantly lower in headache controls compared to patients with IIH (Cohen's $d=0.560$, 95% CI 6.50–75.79; $p=0.021$). The left optic nerve RD values were significantly higher in headache controls compared to patients with IIH (Cohen's $d=-0.676$, 95% CI −219.13 to −43.50; $p=0.004$).

The right optic nerve FA values were significantly lower in headache controls compared to patients with IIH (Cohen's $d=0.568$, 95% CI 8.15–72.00; $p=0.015$).

After multiple comparison corrections, FA and RD values of the left cingulum, AD values of the left and right superior cerebellar peduncle, ADC values of the left middle cerebellar peduncle, ADC and RD values of the left optic nerve, and FA values of the right optic nerve were still statistically significant (Table 2).

The DTI parameters of the patients with IIH and headache controls are summarized in Tables 2 and S2.

Correlation between the CSF opening pressure and DTI parameters in the 42 patients with IIH

There was a positive correlation between the left superior longitudinal fasciculus ADC values and right superior longitudinal fasciculus ADC values and CSF opening pressure ($r=0.43$, $p=0.005$, $r=0.31$, $p=0.044$; respectively).

There was a positive correlation between the genu of the corpus callosum ADC values and CSF opening pressure ($r=0.35$, $p=0.024$).

There was a positive correlation between the left inferior longitudinal fasciculus ADC values and CSF opening pressure ($r=0.39$, $p=0.010$).

There was a positive correlation between the left optic radiation RD and CSF opening pressure ($r=0.31$, $p=0.047$). A positive correlation was detected between the right optic radiation ADC values and CSF opening pressure ($r=0.41$, $p=0.007$) (Table 3, Figure 5).

Compared to patients without papilledema, patients with papilledema showed no significant difference in all DTI parameters ($p>0.05$).

Correlation between the ophthalmological measurements and DTI parameters in the 42 patients with IIH

A positive correlation was found between the Frisen grade of papilledema and RNFL thickness ($r=0.63$, $p<0.001$). A positive correlation was also found between the Frisen grade of papilledema and PSD values ($r=0.37$, $p=0.016$). A negative correlation was found between the PSD and MD values ($r=-0.80$, $p<0.001$).

TABLE 1 Demographics and clinical characteristics of the patients with idiopathic intracranial hypertension and headache control group.

Characteristic	Patients with IIH ($n=42$)	Headache control group ($n=36$)	p
Age, years, mean, (SD)	38.1 (8.9)	38.1 (9.4)	0.977
Sex, *n* (%)			0.015
Female	39 (92.8)	26 (72.2)	
Male	3 (7.2)	10 (27.8)	
Body mass index, kg/m^2, mean (SD)	25.2 (1.9)	23.3 (1.5)	<0.001
Symptoms, *n* (%)			
Headache	40 (95)		
Nausea	10 (23)		
Dizziness	6 (14)		
Tinnitus	11 (26)		
Transient visual obscuration	8 (19)		
Blurred vision	18 (43)		
Diplopia	2 (5)		
Bilateral papilledema, *n* (%)			
Yes	31 (73)		
No	11 (26)		
CSF opening pressure, mm, median (IQR)	350.00 (300.00–390.00)		
Frisen grade of papilledema (right eye), *n* (%)			
Grade 0	15 (36)		
Grade I	11 (26)		
Grade II	9 (21)		
Grade III	3 (7)		
Grade IV	4 (10)		
Frisen grade papilledema (left eye), *n* (%)			
Grade 0	13 (31)		
Grade I	14 (33)		
Grade II	9 (21)		
Grade III	2 (5)		
Grade IV	4 (10)		
Ophthalmological measurements, median (IQR)			
RNFL (worst affected eye), μm, median (IQR)	110.5 (104–136)		
MD (worst affected eye), dB, median (IQR)	−4.58 (−6.82 to −3.64)		
PSD (worst affected eye), dB, median (IQR)	2.80 (2.37–6.15)		
Ocular MRI findings, *n* (%)			
Posterior optic globe flattening	39 (92)		
Optic nerve head protrusion	16 (38)		
Optiv nerve tortuosity	38 (90)		

Note: Data are presented as mean (SD) for normally distributed continuous data, median (IQR) for non-normally distributed continuous data and number of cases (percentage) for categorical variables.

Abbreviations: CSF, cerebrospinal fluid; IIH, idiopathic intracranial hypertension; IQR, interquartile range (25th–75th percentile); MD, mean deviation; PSD, pattern standard deviation; RNFL, retinal nerve fiber layer; SD, standard deviation.

There was a positive correlation between the RNFL thickness and the ADC values of the optic nerve ($r=0.32$, $p=0.039$) (Figure 6).

We did not find any statistically significant differences between the Frisen grade of papilledema, PSD and MD values, and DTI parameters of the optic nerves ($p>0.05$).

DISCUSSION

In the present study, we demonstrated DTI parameter alterations in several white matter tracts, including the cingulum and superior and middle cerebellar peduncle. Previous DTI studies mainly focused on

TABLE 2 Comparison of diffusion tensor imaging parameters between patients with idiopathic intracranial hypertension and headache control group.

	Patients with IIH ($n=42$), mean (SD)	Headache control group ($n=36$), mean (SD)	Mean difference (95% CI)	Cohen's *d*	*p*
FA_Left cingulum	0.505 (0.087)	0.559 (0.068)	53.71 (18.68 to 88.74)	0.681	0.003*
RD_Left cingulum	0.569 (0.073)	0.517 (0.070)	−51.15 (−83.72 to −18.57)	−0.710	0.002*
FA_Right anterior limb internal capsule	0.468 (0.61)	0.496 (0.061)	28.11 (0.11 to 56.11)	0.454	0.049
RD_Right anterior limb internal capsule	0.548 (0.049)	0.521 (0.059)	−27.59 (−52.28 to −2.90)	−0.506	0.029
AD_Left superior cerebellar peduncle	1.576 (0.163)	1.744 (0.188)	168.56 (89.19 to 247.93)	0.961	<0.001*
AD_Right superior cerebellar peduncle	1.637 (0.173)	1.740 (0.166)	103.23 (26.33 to 180.13)	0.607	0.009*
ADC_Left middle cerebellar peduncle	0.732 (0.041)	0.711 (0.034)	−21.66 (−39.04 to −4.28)	−0.564	0.015*
ADC_Left optic nerve	1.430 (0.202)	1.309 (0.199)	−121.37 (−212.40 to −30.33)	−0.603	0.010*
FA_Left optic nerve	0.379 (0.054)	0.420 (0.090)	41.25 (6.50 to 75.79)	0.560	0.021
RD_Left optic nerve	1.130 (0.187)	0.999 (0.201)	−131.31 (−219.13 to −43.50)	−0.676	0.004*
FA_Right optic nerve	0.376 (0.058)	0.416 (0.082)	40.07 (8.15 to 72.00)	0.568	0.015*

Abbreviations: AD, axial diffusivity; ADC, apparent diffusion coefficient; CI, confidence interval; FA, fractional anisotropy; IIH, idiopathic intracranial hypertension; RD, radial diffusivity, SD, standard deviation.

*Shows statistically significant results after multiple comparison correction.

TABLE 3 Correlation between the diffusion tensor imaging parameters and cerebrospinal fluid opening pressure.

	CSF opening pressure	
DTI parameters	(*r*) coef.	*p*
ADC_Left superior longitudinal fasciculus	0.43	0.005
ADC_Right superior longitudinal fasciculus	0.31	0.044
ADC_Genu of corpus callosum	0.35	0.024
ADC_Left inferior longitudinal fasciculus	0.39	0.010
RD_Left optic radiation	0.31	0.047
ADC_Right optic radiation	0.41	0.007

Abbreviations: ADC, apparent diffusion coefficient; CSF, cerebrospinal fluid; RD, radial diffusivity.

white matter changes in the periventricular white matter.[17] According to their hypothesis, patients with IIH may experience aberrant CSF pressure pulses linked to elevated ICP, which could result in mechanical compression against the lateral ventricle wall. This compression could cause tissue compaction, altering the axonal organization in the periventricular white matter tissue microstructure.[17] Sarica et al.[17] pointed out the morphological differences in the periventricular white matter microstructure in patients with IIH, particularly in the corona radiata and corpus callosum. They found decreased MD, RD, and AD values in these white matter microstructures. Contrary to this previous study, we detected no significant change in the DTI metrics in the periventricular white matter. However, we demonstrated positive correlations between the ADC values of the genu of the corpus callosum and superior longitudinal fasciculus and CSF opening pressure in patients with IIH. We speculate that recurrent pressure pulsations brought on by high CSF pressure mechanically press against the lateral ventricle wall. The genu of the corpus callosum, which is thought to link the bilateral prefrontal cortices of the cerebral hemispheres, is involved in several motor, perceptual, and cognitive processes. Moreover, the ipsilateral frontal cortices and the parietal, occipital, and temporal lobes are connected by a large bundle of association fibers called the superior longitudinal fasciculus, located in the white matter of each cerebral hemisphere. The superior longitudinal fasciculus facilitates the development of a bidirectional neural network, which is required for essential functions, including attention, memory, emotions, and language.[19] Increased ADC values in these white matter microstructures could be a sign of myelin damage, such as a reduction in myelin content or demyelination, resulting in an expansion of the extracellular space due to increased CSF pressure. In line with our findings, Grech et al.[20] reported that patients with IIH were significantly impaired in sustained attention and executive function compared to controls. Kharkar et al.[21] demonstrated borderline deficits in memory, learning, executive function, visuospatial skills, and language in patients with IIH. Moreover, the inferior longitudinal fasciculus is an important ventral associative bundle that links and transmits data between the temporal and occipital lobes. It has been hypothesized that the inferior longitudinal fasciculus's placement permits rapid visual information transfer.[22] We may speculate that increased ADC values in the inferior longitudinal fasciculus correlated with increased CSF pressure may be linked to visual problems in patients with IIH.

In this study, we found decreased FA and increased RD values in the cingulum in patients with IIH. The cingulum bundle runs

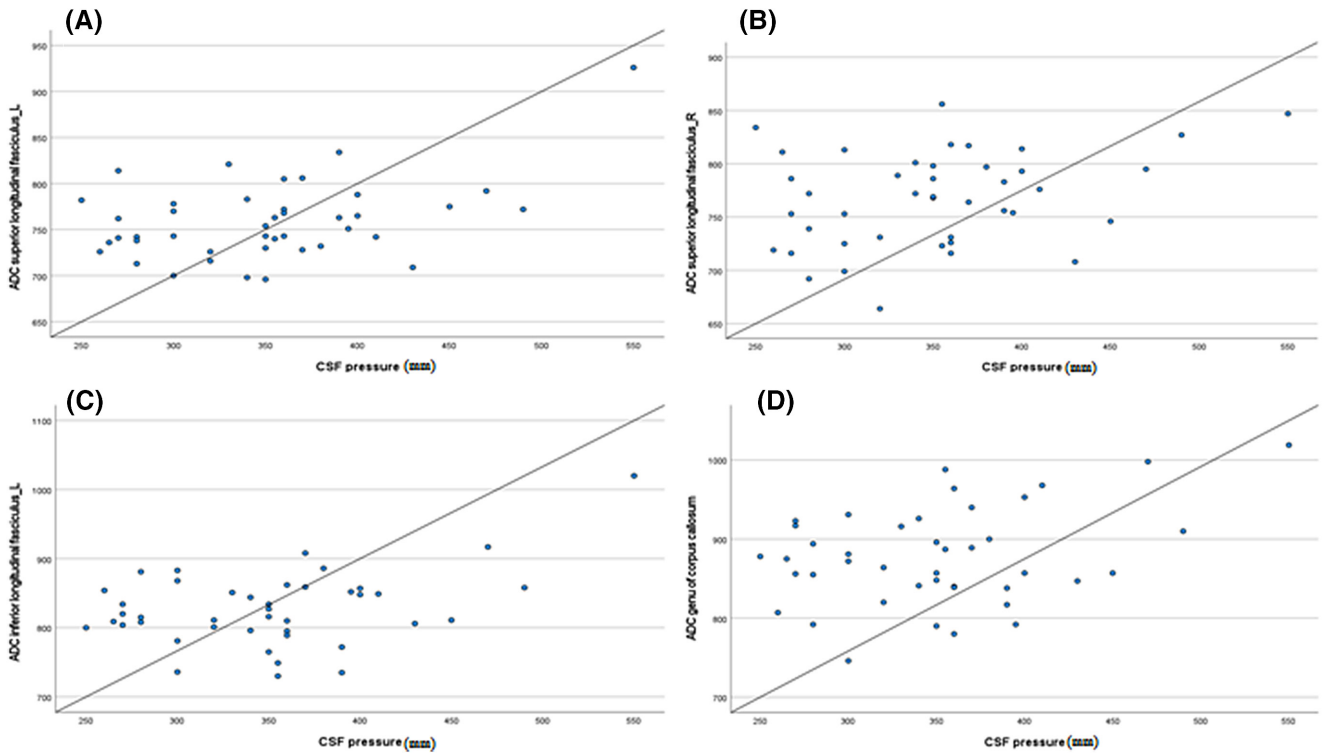

FIGURE 5 Scatter plots show the relationship between diffusion tensor imaging parameters and cerebrospinal fluid (CSF) opening pressure. Significant results were detected in the apparent diffusion coefficient (ADC) values of the left superior longitudinal fasciculus (A), right superior longitudinal fasciculus (B), left inferior longitudinal fasciculus (C) and genu of corpus callosum (D). [Color figure can be viewed at wileyonlinelibrary.com]

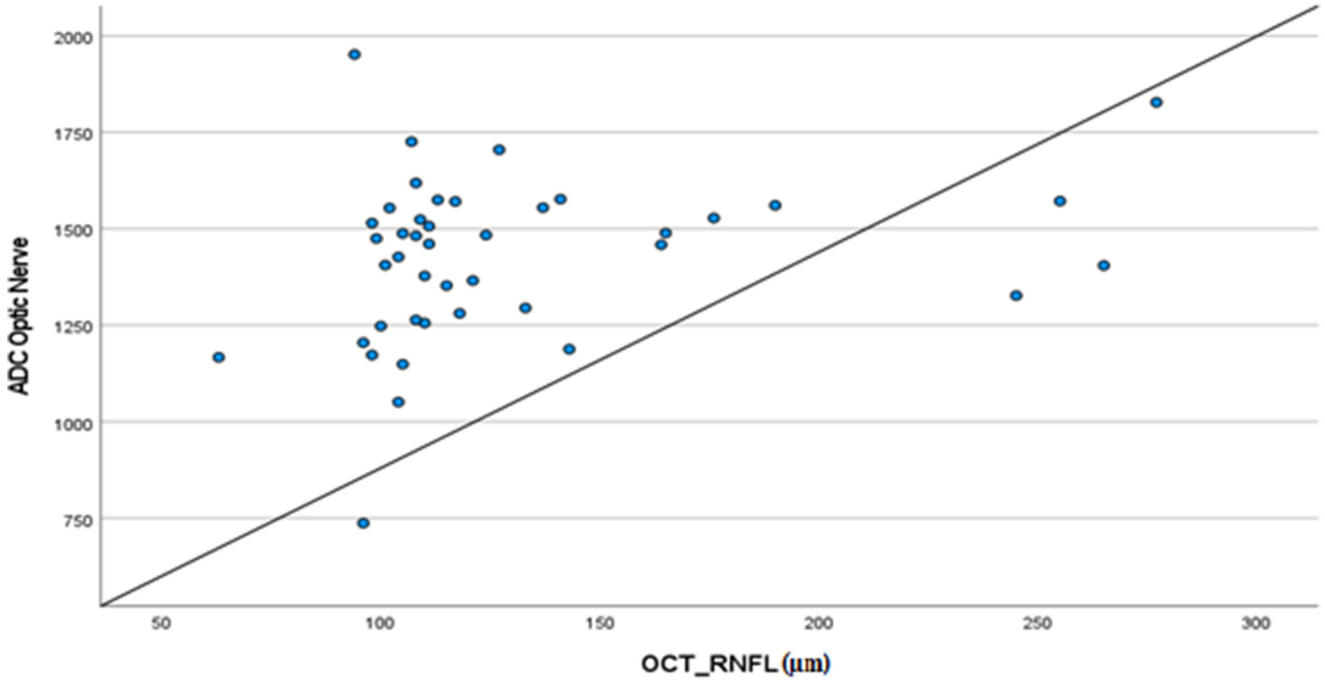

FIGURE 6 Scatter plot shows the relationship between diffusion tensor imaging parameters and retinal nerve fiber layer (RNFL) thickness. Significant results were detected in the apparent diffusion coefficient (ADC) values of the optic nerve. [Color figure can be viewed at wileyonlinelibrary.com]

longitudinally over the corpus callosum and forms the basis of the cingulate cortex. The medial frontal gyrus, cuneate, lingual, posterior parietal, and fusiform gyri are all connected to the cingulate cortex by short-range fibers in the cingulum bundle. The cingulum bundle controls emotion, episodic memory, spatial processing, and attention-shifting tasks.[23–27] We hypothesized that the reduction

of FA in the cingulum bundle could be explained by mechanical pressure on the fibers causing axonal degeneration, while an increase in RD would suggest myelin sheath degradation. Zur et al.[28] demonstrated multidomain cognitive impairment in patients with IIH, including non-verbal memory, motor skills, executive function, visual–spatial processing, information processing, speed attention, and problem-solving. In addition to the cingulum, this is the first study to reveal the effects of increased CSF pressure on superior and middle cerebellar peduncle integrity in patients with IIH. The superior and middle cerebellar peduncle are crucial in transmitting output signals from the cerebellum to other parts of the central nervous system. It is involved in motor control and coordination, contributing to the smooth execution of voluntary movements.[29] A decrease in AD could suggest axonal injury in the superior cerebellar peduncle, whereas higher ADC values in the middle cerebellar peduncle could be a sign of myelin damage in patients with IIH in our study. The DTI alterations we detected in our study demonstrate that white matter injury in patients with IIH extends beyond the periventricular deep white matter.

Several epidemiological studies have demonstrated a significant correlation between IIH and obesity. These studies reported that ~90% of patients with IIH are overweight, as in our study.[30,31] Obesity and being female are two identified risk factors for IIH. These findings raise the possibility of a role for sex hormones and substances generated by adipose tissue, such as adipokines, which are cytokines primarily secreted by adipose tissue and may impact CSF dynamics.[31] Although there is not a single, cohesive explanation of how IIH develops, dysregulation of ICP is an important area of research interest. A previous neuropathological study reported altered mitochondrial morphology in perivascular astrocytic endfeet and neurons of patients with IIH. This finding may imply that IIH entails pathological alterations in the brain's cells at the cellular level in addition to CSF disruption.[32]

Previous DTI studies in hydrocephalus showed a relationship between altered diffusion metrics and high CSF pressure.[33,34] In patients with normal pressure hydrocephalus (NPH), increased ADC and decreased FA values were depicted in the periventricular white matter and corpus callosum by several DTI studies.[33,34] These alterations were explained by several mechanisms, including ventricular enlargement, periventricular interstitial edema, and reduced CSF turnover, with an accumulation of neurotoxic substances resulting in axonal loss and wallerian degeneration. A neuropathological study demonstrated the evidence of changed mitochondria phenotypes in neurons in patients with idiopathic NPH, which may suggest defective cellular clearance in patients with idiopathic NPH and may contribute to neurodegeneration.[35] Moreover, DTI changes were reported in the internal capsule and corticospinal tracts in patients with NPH, indicating that the white matter microstructural changes were extended beyond the periventricular white matter, similar to our study.[33]

Visual disturbances are among the primary signs of IIH. They are commonly a direct result of papilledema, which is caused by an increased ICP. In our study, we found increased ADC and RD values and decreased FA values in the optic nerve. The alteration in the DTI metrics may indicate that high ICP impacts the microstructural integrity of the optic nerve due to pressure-induced tissue compression. Reduced FA values could signify a dismyelination process and axonal fiber loss. Myelin sheath irregularity, resulting in lower cellularity or axon number and increased extracellular water mobility/diffusivity, may explain increased ADC values. Moreover, increased RD values may suggest myelin sheath degradation. These findings may indicate myelin sheath damage and axonal disruption in the optic nerves of patients with IIH. Schmidt et al.[18] demonstrated decreased FA values in the optic nerve in patients with IIH, similar to our study. They speculated that these microstructural changes may be the underlying reason for the functional deterioration of the optic nerve. Another DTI study reported increased MD and decreased FA values in optic discs in patients with IIH.[36] They pointed out that reduced cellularity and loss of cell membrane integrity with free space for water molecule diffusion may cause higher MD values of the optic disc in patients. Lower FA values may result from decreased anisotropy and weakened water molecule diffusion directions brought on by swelling and disc edema. In addition, we found a positive correlation between the CSF pressure and RD values of the optic radiation, which may indicate a demyelination process beyond the optic nerve in the optic pathways. Interestingly, we did not identify a correlation between microstructural abnormalities and papilledema.

To the best of our knowledge, our study is the first to evaluate the correlation between the RNFL thickness, Frisen grade of papilledema, PSD and MD values, and DTI parameters of the optic nerves. A previous DTI study pointed out significant differences in FA and MD values of the optic disc between patients with IIH with early and advanced papilledema and visual field defects.[36] Another DTI study demonstrated a significant difference in DTI parameters of the optic nerve and optic radiation in patients with early and severe glaucoma and correlated them with RNFL thickness.[37] They explained these results by attributing papilledema on the optic disc and optic nerve to elevated intraocular pressure. Ahuja et al.[38] reported statistically significant thickening of the RNFL in patients with papilledema in comparison to controls. In addition, they reported positive correlation between Frisen grading of papilledema and RNFL thickness measurements, similar to our study. In our study, we found a positive correlation between the RNFL thickness and ADC values of the optic nerve. Reduced cellularity and increased extracellular water mobility/diffusivity may explain increased ADC values. Increased ADC values may be attributed to the swelling and edema of the optic nerve due to increased ICP, which correlates with the nerve fiber layer (RNFL) thickness in our study.

A major strength of our study is that, unlike the literature, we demonstrated that IIH is associated with microstructural integrity in several white matter tracts beyond the periventricular white matter; however, this study includes certain drawbacks. First, it should be emphasized that DTI results show eigenvectors of diffusing water molecules through the complexity of the tracts, which may provide insight into the microstructural integrity rather than directly measuring the integrity of the white matter. Furthermore, measurement reproducibility may be reduced because the ROI-based approach

depends on the operator. We suggest that future research use the tract-based spatial statistics method to address the drawbacks of the ROI-based approach. Another drawback is that, for ethical reasons, no LP was done in the control group. We did not evaluate the patients after treatment-induced reductions in ICP, which was one of the potential limitations of our study. Another limitation is that, while statistically higher compared to the headache control group, the BMI values of the patients with IIH were considerably lower than those reported in the literature. Due to the nature of the retrospective study, the headache control group had male predominance, and there was a sex imbalance between the groups in our study. Another potential limitation of our study is the relatively small sample size. Long-term cohort studies with larger patient populations will be crucial in clarifying how elevated ICP affects white matter integrity and optic pathways in patients with IIH.

CONCLUSION

The present study highlights that IIH can be associated with deteriorated DTI values, which might be interpreted as a sign of impaired white matter microstructural integrity in many brain regions beyond the periventricular white matter. We postulated that pressure-induced edema and axonal degeneration may be the potential underlying mechanisms of this microstructural damage. Moreover, increased ICP impacts the microstructural integrity of the optic nerve due to pressure-induced tissue compression. Future studies will need to elucidate the role of elevated ICP, in contributing to microstructural damage in the white matter structures, and whether the changes in patients with IIH can be reversed by returning their ICP to normal levels.

AUTHOR CONTRIBUTIONS

Bahar Atasoy: Conceptualization; data curation; investigation; methodology; supervision; writing – original draft; writing – review and editing. **Asli Yaman Kula:** Data curation; investigation; methodology; writing – review and editing. **Serdar Balsak:** Data curation; formal analysis; investigation; writing – review and editing. **Yagmur Basak Polat:** Data curation; methodology; writing – original draft. **Zeynep Donmez:** Conceptualization; formal analysis; writing – review and editing. **Ahmet Akcay:** Data curation; writing – original draft. **Abdusselim Adil Peker:** Formal analysis; writing – review and editing. **Ozlem Toluk:** Formal analysis; methodology. **Alpay Alkan:** Conceptualization; supervision; writing – review and editing.

ACKNOWLEDGMENTS

We would like to thank Dr. Furkan Kırık, who made the ophtalmalogical measurements and shared this data for this study.

CONFLICT OF INTEREST STATEMENT

Bahar Atasoy, Asli Yaman Kula, Serdar Balsak, Yagmur Basak Polat, Zeynep Donmez, Ahmet Akcay, Abdusselim Adil Peker, Ozlem Toluk and **Alpay Alkan** declare no conflict of interest.

ORCID

Bahar Atasoy https://orcid.org/0000-0002-5393-5876
Asli Yaman Kula https://orcid.org/0000-0001-8857-9210
Serdar Balsak https://orcid.org/0000-0001-8765-4418
Yagmur Basak Polat https://orcid.org/0000-0003-1410-7303
Zeynep Donmez https://orcid.org/0000-0002-0030-3250
Ahmet Akcay https://orcid.org/0000-0001-7016-6004
Ozlem Toluk https://orcid.org/0000-0001-6495-0839
Alpay Alkan https://orcid.org/0000-0002-3002-1641

REFERENCES

1. Friedman DI, Liu GT, Digre KB. Revised diagnostic criteria for the pseudotumor cerebri syndrome in adults and children. *Neurology*. 2013;81(13):1159-1165.
2. Hoffmann J, Kreutz KM, Csapó-Schmidt C, et al. The effect of CSF drain on the optic nerve in idiopathic intracranial hypertension. *J Headache Pain*. 2019;20(1):59.
3. Thaller M, Mytton J, Wakerley BR, Mollan SP, Sinclair AJ. Idiopathic intracranial hypertension: evaluation of births and fertility through the hospital episode statistics dataset. *BJOG*. 2022;129(12):2019-2027.
4. Durcan FJ, Corbett JJ, Wall M. The incidence of pseudotumor cerebri. Population studies in Iowa and Louisiana. *Arch Neurol*. 1988;45(8):875-877.
5. Radhakrishnan K, Ahlskog JE, Cross SA, Kurland LT, O'Fallon WM. Idiopathic intracranial hypertension (pseudotumor cerebri). Descriptive epidemiology in Rochester, Minn, 1976 to 1990. *Arch Neurol*. 1993;50(1):78-80.
6. Radhakrishnan K, Thacker AK, Bohlaga NH, Maloo JC, Gerryo SE. Epidemiology of idiopathic intracranial hypertension: a prospective and case-control study. *J Neurol Sci*. 1993;116(1):18-28.
7. Kesler A, Stolovic N, Bluednikov Y, Shohat T. The incidence of idiopathic intracranial hypertension in Israel from 2005 to 2007: results of a nationwide survey. *Eur J Neurol*. 2014;21(8):1055-1059.
8. Asensio-Sanchez VM, Merino-Angulo J, Martínez-Calvo S, Calvo MJ, Rodríguez R. Epidemiology of pseudotumor cerebri. *Arch Soc Esp Oftalmol*. 2007;82:219-222.
9. Fargen K, Coffman S, Torosian T, Brinjikji W, Nye B, Hui F. "Idiopathic" intracranial hypertension: an update from neurointerventional research for clinicians. *Cephalalgia*. 2023;43(4):033310242311613.
10. Degnan A, Levy L. Pseudotumor cerebri: brief review of clinical syndrome and imaging findings. *AJNR Am J Neuroradiol*. 2011;32(11):1986-1993.
11. Suzuki H, Takanashi J, Kobayashi K, Nagasawa K, Tashima K, Kohno Y. MR imaging of idiopathic intracranial hypertension. *AJNR Am J Neuroradiol*. 2001;22(1):196-199.
12. Zagardo M, Cail W, Kelman S, Rothman M. Reversible empty Sella in idiopathic intracranial hypertension: an indicator of successful therapy? *AJNR Am J Neuroradiol*. 1996;17(10):1953-1956.
13. Bialer O, Rueda M, Bruce B, Newman N, Biousse V, Saindane A. Meningoceles in idiopathic intracranial hypertension. *AJR Am J Roentgenol*. 2014;202(3):608-613.
14. Kwee R, Kwee T. Systematic review and meta-analysis of MRI signs for diagnosis of idiopathic intracranial hypertension. *Eur J Radiol*. 2019;116:106-115.
15. Jones DK, Leemans A. Diffusion tensor imaging. *Methods Mol Biol*. 2011;2011:127-144.
16. Mori S, Zhang J. Principles of diffusion tensor imaging and its applications to basic neuroscience research. *Neuron*. 2006;2006:527-539.
17. Sarica A, Curcio M, Rapisarda L, Cerasa A, Quattrone A, Bono F. Periventricular white matter changes in idiopathic intracranial hypertension. *Ann Clin Transl Neurol*. 2019;6(2):233-242.

18. Schmidt C, Wiener E, Lüdemann L, et al. Does IIH alter brain microstructures? A DTI-based approach. *Headache*. 2017;57(5):746-755.
19. Kamali A, Flanders AE, Brody J, Hunter JV, Hasan KM. Tracing superior longitudinal fasciculus connectivity in the human brain using high resolution diffusion tensor tractography. *Brain Struct Funct*. 2014;219(1):269-281.
20. Grech O, Clouter A, Mitchell JL, et al. Cognitive performance in idiopathic intracranial hypertension and relevance of intracranial pressure. *Brain Commun*. 2021;3(3):fcab202.
21. Kharkar S, Hernandez R, Batra S, et al. Cognitive impairment in patients with pseudotumor cerebri syndrome. *Behav Neurol*. 2011;24:143-148.
22. Shin J, Rowley J, Chowdhury R, et al. Inferior longitudinal Fasciculus' role in visual processing and language comprehension: a combined MEG-DTI study. *Front Neurosci*. 2019;13:875.
23. Brunet-Gouet E, Decety J. Social brain dysfunctions in schizophrenia: a review of neuroimaging studies. *Psychiatry Res*. 2006;148:75-92.
24. Fitzsimmons J, Rosa P, Sydnor VJ, et al. Cingulum bundle abnormalities and risk for schizophrenia. *Schizophr Res*. 2020;215:385-391.
25. Fan YT, Fang YW, Chen YP, et al. Aging, cognition, and the brain: effects of age-related variation in white matter integrity on neuropsychological function. *Aging Ment Health*. 2019;23(7):831-839.
26. Bennett IJ, Madden DJ, Vaidya CJ, Howard DV, Howard JH Jr. Age-related differences in multiple measures of white matter integrity: a diffusion tensor imaging study of healthy aging. *Hum Brain Mapp*. 2010;31(3):378-390.
27. Bubb EJ, Metzler-Baddeley C, Aggleton JP. The cingulum bundle: anatomy, function, and dysfunction. *Neurosci Biobehav Rev*. 2018;92:104-127.
28. Zur D, Naftaliev E, Kesler A. Evidence of multidomain mild cognitive impairment in idiopathic intracranial hypertension. *J Neuroophthalmol*. 2015;35(1):26-30.
29. Imai T, Sakamoto K, Hasegawa T, et al. Cerebellar peduncle damage in Langerhans cell histiocytosis-associated neurodegenerative disease revealed by diffusion tensor imaging. *Neuroradiology*. 2023;66:43-54.
30. Markey KA, Mollan SP, Jensen RH, Sinclair AJ. Understanding idiopathic intracranial hypertension: mechanisms, management, and future directions. *Lancet Neurol*. 2016;15(1):78-91.
31. Hussein M, Abdelghaffar M, Ali M, Yassein AM, Khalil DM, Magdy R. Impact of Ramadan fasting on vision and headache-related quality of life in women with idiopathic intracranial hypertension: a prospective observational study. *Headache*. 2024;64(4):352-360.
32. Eide PK, Hasan-Olive MM, Hansson HA, Enger R. Increased occurrence of pathological mitochondria in astrocytic perivascular endfoot processes and neurons of idiopathic intracranial hypertension. *J Neurosci Res*. 2021;99(2):467-480.
33. Hattori T, Ito K, Aoki S, et al. White matter alteration in idiopathic normal pressure hydrocephalus: tract-based spatial statistics study. *AJNR Am J Neuroradiol*. 2012;33(1):97-103.
34. Atasoy B, Aralasmak A, Cetinkaya E, et al. Normal pressure hydrocephalus: clinical symptoms, cerebrospinal fluid flow metrics and white matter changes. *J Comput Assist Tomogr*. 2020;44(1):59-64.
35. Hasan-Olive MM, Enger R, Hansson HA, Nagelhus EA, Eide PK. Pathological mitochondria in neurons and perivascular astrocytic endfeet of idiopathic normal pressure hydrocephalus patients. *Fluids Barriers CNS*. 2019;16(1):39.
36. Razek AAKA, Batouty N, Fathy W, Bassiouny R. Diffusion tensor imaging of the optic disc in idiopathic intracranial hypertension. *Neuroradiology*. 2018;60(11):1159-1166.
37. Sidek S, Ramli N, Rahmat K, Ramli NM, Abdulrahman F, Tan LK. Glaucoma severity affects diffusion tensor imaging (DTI) parameters of the optic nerve and optic radiation. *Eur J Radiol*. 2014;83:1437-1441.
38. Ahuja S, Anand D, Dutta TK, Roopesh Kumar VR, Kar SS. Retinal nerve fiber layer thickness analysis in cases of papilledema using optical coherence tomograph—a case control study. *Clin Neurol Neurosurg*. 2015;136:95-99.

SUPPORTING INFORMATION

Additional supporting information can be found online in the Supporting Information section at the end of this article.

How to cite this article: Atasoy B, Yaman Kula A, Balsak S, et al. Role of diffusion tensor imaging in the evaluation of white matter integrity in idiopathic intracranial hypertension. *Headache*. 2024;64:1076-1087. doi:10.1111/head.14825